LBL-38074

OPTICAL INDICES OF TIN-DOPED INDIUM OXIDE AND TUNGSTEN OXIDE ELECTROCHROMIC COATINGS

K. VON ROTTKAY, M. RUBIN, N.OZER
Lawrence Berkeley National Laboratory, University of California, Berkeley CA 94720, Nik_von_Rottkay@ccmail.lbl.gov, MDRubin@LBL.gov, NOzer@LBL.gov

ABSTRACT

Thin films of tin-doped indium oxide are widely used for transparent conductors. One application of In_2O_3:Sn (ITO) is transparent contacts for electrochromic electrodes. Optical design of electrochromic devices requires knowledge of the optical constants for each layer from the near ultraviolet and visible to the mid infrared. Determination of the optical constants of the electrochromic layer cannot be made in isolation; a complete device or at least a half-cell including a layer of ITO is required to change the optical state of the electrochromic material. Measurements on ITO were made using variable-angle spectral ellipsometry, and spectral transmittance and reflectance. A series of structural models were fit to this data. The problem is complicated because of inhomogeneity in the films, variability in the manufacturing process, and sensitivity to environmental conditions. The spectral dependency was modeled by a single Lorentz oscillator and a Drude free-electron component. This data was then used as the basis for a model to extract the optical constants for a tungsten oxide electrochromic film.

INTRODUCTION

Electrochromic devices are being developed for windows, mirrors, displays and other applications. Design of the optical properties requires the knowledge of the optical constants of the individual layers in the device. Before turning to the electrochromic layers themselves, we must first study the optical properties of the transparent conducting contact layers on which the electrochromic materials are grown. One of the most widely used transparent conductors is tin-doped indium oxide In_2O_3:Sn which is often called indium tin oxide or ITO.

ITO films can have a wide range of properties depending on deposition method and parameters [1]. For example, Kane, Schweizer and Kern [2] found that the refractive index for CVD ITO films on Si varied over a great range from 1.58 to 2.48 at 546 nm. Bright [3] also found a wide range of values for films deposited by evaporation and sputtering on glass and flexible polyester substrates. This in itself is not surprising; variations in dopant and carrier concentration should produce large variations in optical constants, especially in the infrared. The doping or vacancy concentrations are so heavy in these materials that the compositional change alone might be enough to affect the visible properties. It is clear that a useful compilation of properties should include a range of compositions or sheet resistance; a time-consuming but straightforward task.

A more troublesome problem arises because of variations among films of a type. For example, Hamberg and Granqvist [4] find significant differences even in films produced under nominally identical conditions. Furthermore, ITO films can be so sensitive to environmental conditions that they have found use as gas sensors [5].

Considering for the moment only the determination of properties of a given film at a given time, analysis of these films is still relatively difficult compared to many other materials. Carniglia [6] recently determined the index of refraction of sputtered ITO from reflectance and transmittance measurements at normal incidence. For the range from 300-850 nm only, he found it necessary to use a gradient index model and an extra term in the empirical Cauchy dispersion formula to obtain good fits to the index. Bright [3] used similar measurements and a combined Drude/Lorentz model to obtain a good fit in at least one case. Hamberg and Granqvist [4] using a

homogeneous structural model found that a frequency dependent relaxation time in the Drude model was required for good agreement with their radiometric data.

The optical properties of a commercial grade of ITO are carefully measured by both radiometry and ellipsometry. Several plausible models of the underlying optical response and the layer structure are constructed. The models are examined by fitting the optical data to each. Finally, the data for the conducting layer is used to construct a model in which the properties of a WO_3 top layer are unknown. The properties of the WO_3 are then determined in turn.

METHODS

The optical properties are measured using both ellipsometric and radiometric techniques. A variable-angle spectroscopic ellipsometer by J.A Woollam Co. is used over the extended visible range (300-1000 nm).

Transmittance and reflectance measurements are made over the solar spectrum from 300-2500 nm. All measurements were made at normal incidence using either a Perkin-Elmer Lambda 9 or Lambda 19 spectrophotometer. For these highly specular samples, the detectors could be exposed directly, rather than together with an integrating sphere. This detector arrangement provides maximum accuracy and also permits the backsurface to be roughened, which would otherwise contribute to the integrating sphere signal. Reflectance measurements were made with relative reflectance attachment with an angle of incidence of 8 degrees. A front-surface Al mirror calibrated by NIST was used as a reference. As a further check, measurements were made at 670 nm using a feedback-stabilized laser diode with a short coherence length and a large-area silicon detector. The error for this system is typically 0.1%.

Some of the surface features of the structural model were verified by atomic force microscopy (AFM) using a Park Scientific Instruments Autoprobe. Additional information on compositional variations was obtained at Donnelly Corporation by etching the ITO film. Film thickness was measured in some cases using a Veeco Dektak II surface profilometer.

Ellipsometric and radiometric data were fitted together weighting both data types according to their standard deviations. The standard deviations of the reflectance and transmittance measurements were not directly measured, but had to be assigned by comparison measurements and were taken as 0.1% over the whole spectral range from 300-2500nm . Backside reflections were generally accounted for and included as fit parameters.

In all cases we considered the material to be represented by a superposition of a single Lorentz oscillator and a Drude free-electron component:

$$\varepsilon_1(\omega) = \varepsilon_\infty - \frac{\omega_p^2}{\omega^2+\gamma^2} + \omega_p^2 \frac{\omega_1^2-\omega^2}{\left(\omega_1^2-\omega^2\right)^2+\beta^2\omega^2} = n^2-\kappa^2$$

$$\varepsilon_2(\omega) = \frac{\gamma}{\omega}\frac{\omega_p^2}{\omega^2+\gamma^2} + \omega_p^2 \frac{\beta\omega}{\left(\omega_1^2-\omega^2\right)^2+\beta^2\omega^2} = 2n\kappa$$

where γ and β are damping factors,

$$\omega_p = \sqrt{\frac{N_v e^2}{\varepsilon_0 m_c^*}} \text{ and}$$

$$\omega_1^2 = \omega_0^2 - \frac{N_v e^2}{3\varepsilon_0 m_c^*}$$

with the carrier concentration N_v, the elementary charge e, the vacuum permittivity ε_0 and m_c^* the effective electron mass in the conduction band. Lattice vibrations in the far infrared have been observed, but they are too distant to contribute significantly [4].

RESULTS

Ellipsometric and radiometric data (Figure 1 and Figure 2) was taken from a sample of ITO from Donnelly Corporation made by reactive sputtering onto a glass substrate moving under the sputtering target. The deposition effectively takes place in a single step so that the structure would ideally be represented by a single homogeneous layer (Figure 3). In this oversimplified case, the model does not fit the ellipsometric data of Figure 1 particularly well, especially delta at 57 degrees. Nevertheless, the resulting index data shown in Figure 3 may be useful for approximate calculations.

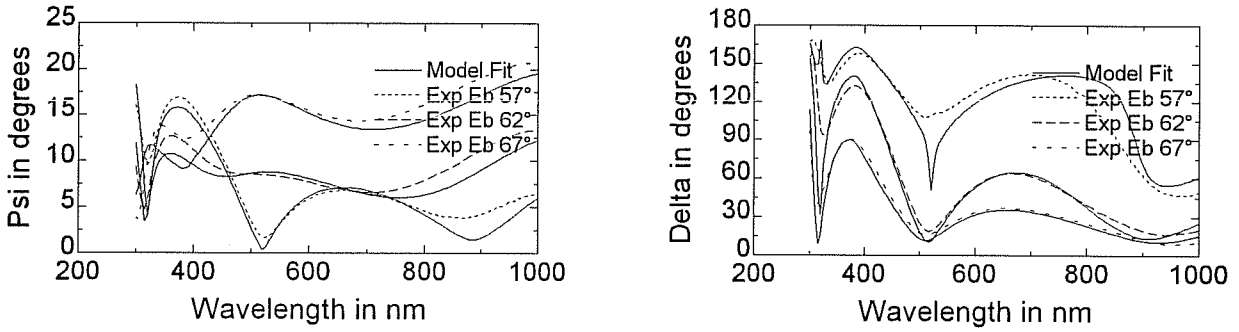

Figure 1. Spectral ellipsometric data at 3 angles (dashed lines) for the ITO film on glass and fitted by the model of Figure 3 (solid lines).

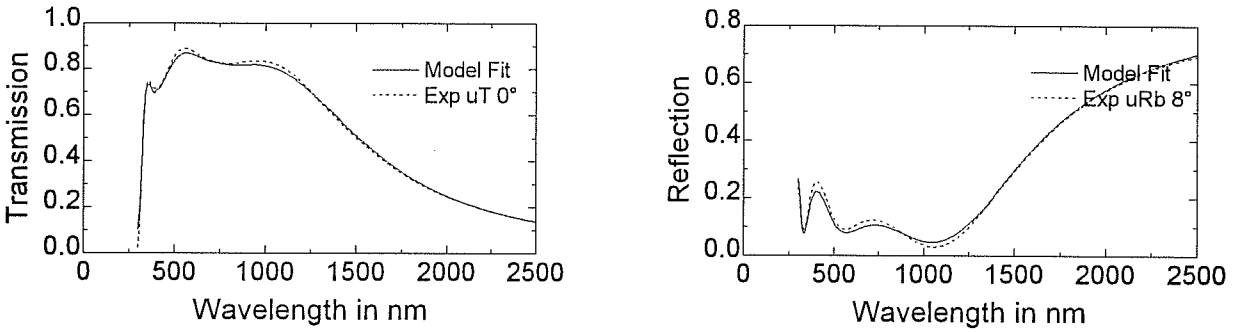

Figure 2. Spectral radiometric data at normal incidence (dashed line) for the ITO film on glass, and fitted by the model of Figure 3 (solid line).

1	ITO	1524.2 Å
0	glass	1.1 mm

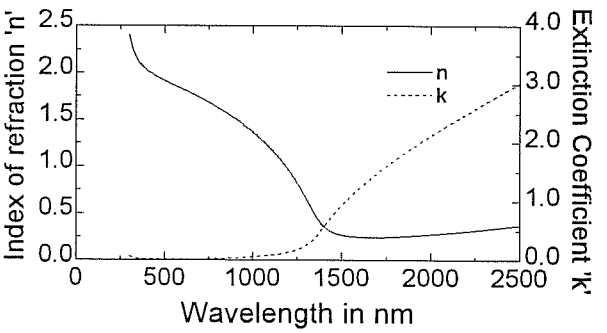

Figure 3. a) structural model and b) optical constants for the film and substrate.

Models with additional independent layers gave improved results and indicated a depth dependent dispersion. As in the case of the dispersion models, use of structural models that simply give the best fit was avoided. Correlation between parameters was very strong, so improvements to the fit were considered dangerous predictors of actual structure. Other independent techniques provide further information about the structure of the film.

Chemical etch experiments show that the film has a higher etch rate near the air and glass interfaces. This indicates that the film is closer to stoichiometry in these regions. The film may have obtained additional oxygen from the glass substrate during formation and from the atmosphere after deposition. Also, as the film passes under the magnetron cathode, it encounters a reduced flux of In at very high angles of deposition. The O_2 partial pressure is fixed, so that the impingement rate of O_2 at the surface is constant. Thus, the bottom and top layers of the film would have a higher oxygen content.

Surface roughness was simulated by a Bruggemann effective medium approximation layer, where a portion of 50% void was included to the ITO top layer. The complex dielectric constant of this EMA layer can be calculated by numerically solving the following equation:

$$\frac{\tilde{\varepsilon}_{ITO}-\tilde{\varepsilon}}{\tilde{\varepsilon}_{ITO}+2\tilde{\varepsilon}}+\frac{\tilde{\varepsilon}_{void}-\tilde{\varepsilon}}{\tilde{\varepsilon}_{void}+2\tilde{\varepsilon}}=0$$

Such a layer added to the model significantly improves the fit and results in a predicted surface roughness of 20 Å in close agreement with direct AFM measurement. The model and index data are shown in Figure 5.

Analysis of AFM images (Figure 4) yields also a surface roughness of 20 Å. In doing this we determined the grain size of the crystallites of the sample as about 100 nm.

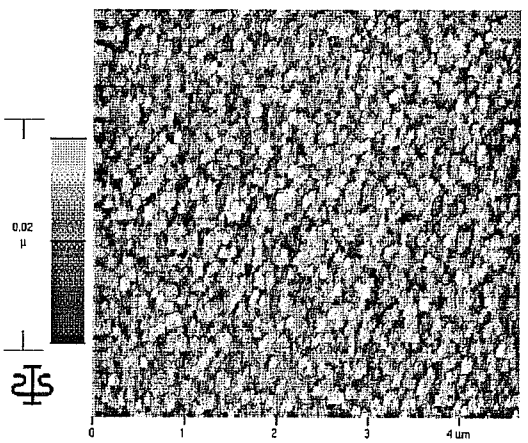

Figure 4

3	EMA (ITO_top)/50% void	20.13 Å
2	ITO_top	744.28 Å
1	ITO_bottom	734.97 Å
0	glass	1.1 mm

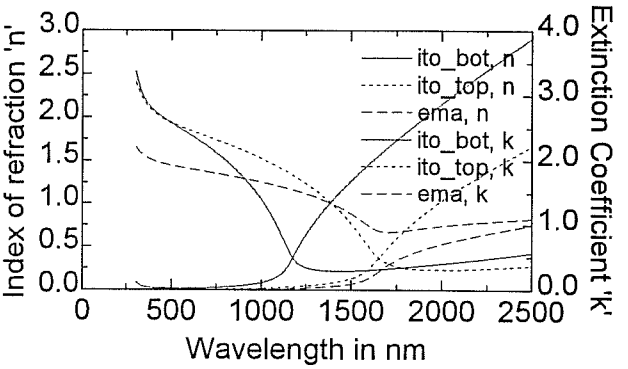

Figure 5. a) structural model and b) optical constants for the layers and substrate.

Example of Electrochromic Coating

It should now be possible to use this data to build a base model of an electrochromic coating on a transparent conductor. Tungsten oxide WO_3 was chosen as an example because it is the most widely used electrochromic material. The sample was deposited by a sol-gel technique using precursors supplied by Donnelly on to a sample of their sputtered ITO. Relatively good fits are obtained to the experimental data using the fixed data for ITO as determined above. In this case a single-layer model results in accurate values for the index of WO_3 (Figure 8).

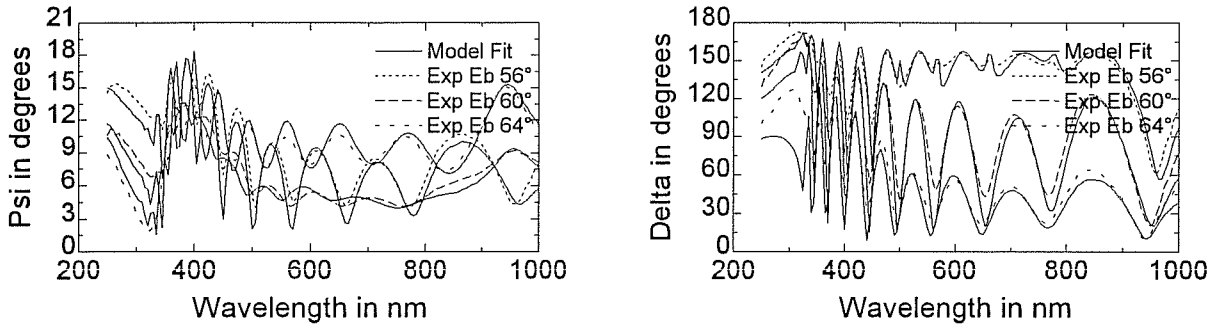

Figure 6. Spectral ellipsometric data at 3 angles (dashed lines) for the WO_3 film on ITO glass and fitted by the model of Figure 8 (solid lines).

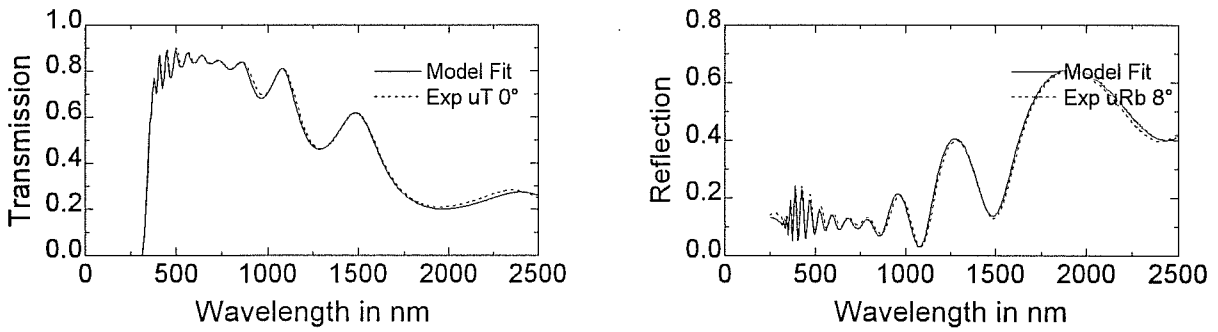

Figure 7. Spectral radiometric data at normal incidence (dashed line) for a WO_3 film on glass, and fitted by the model of Figure 8 (solid line).

4	ema (wo3)/50% void	3.6709 nm
3	wo3	930.97 nm
2	ito_top	73.486 nm
1	ito_bot	76.031 nm
0	glass	1.1 mm

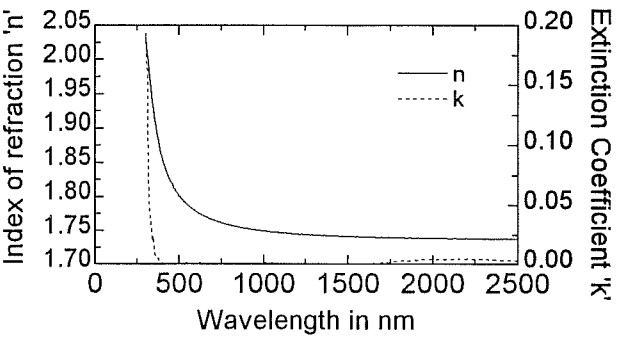

Figure 8. a) structural model and b) optical constants for a WO_3 film on ITO glass.

CONCLUSIONS

The optical constants of ITO can be represented over a wide range of wavelength using a single Lorentz oscillator combined with a Drude free-electron component. Improved results can be obtained by considering structural inhomogeneity and surface roughness. The optical properties of an electrochromic WO_3 film deposited on top of the ITO could be extracted by fixing the In_2O_3:Sn properties.

ACKNOWLEDGMENT

This work was supported by the Assistant Secretary for Energy Efficiency and Renewable Energy, Office of Building Technologies, Building Systems and Materials Division of the US Department of Energy under Contract No. DE-AC03-76SF00098.

REFERENCES

1. G. Frank, E. Kauer, H. Kostlin, and F.J. Schmitte in SPIE Conference. on Optical Coatings for Energy Efficiency and Solar Applications (Los Angeles CA, 1982) p. 29-37.
2. J. Kane, H.P. Schweizer, and W. Kern, Thin Solid Films **29**, p. 155 (1991).
3. C. Bright in Society of Vacuum Coaters, 36th Annual Tech, Conference Proc. p. 63 (1993).
4. I. Hamberg and C.G. Granqvist, J. Appl. Phys. **60** (11), (1986) p 123.
5. G.N. Advani and A.D. Gordon, J. Electron. Mater. **9** (1980) p. 29.
6. C.K. Carniglia, in Society of Vacuum Coaters, 38th Annual Tech, Conference Proc. (1995).
7. C.G. Granqvist, Appl. Phys. A57, (1993) p. 19.